ornl

OAK RIDGE NATIONAL LABORATORY

MARTIN MARIETTA

ORNL/TM-11160

Shield Optimization Program, Part V: A Hydrodynamic Comparison Using HULL and PUFF-TFT for a One-Dimensional Aluminum Slab

M. S. Smith
T. J. Burns
J. O. Johnson

OAK RIDGE NATIONAL LABORATORY
CENTRAL RESEARCH LIBRARY
CIRCULATION SECTION
4500N ROOM 175
LIBRARY LOAN COPY
DO NOT TRANSFER TO ANOTHER PERSON
If you wish someone else to see this report, send in name with report and the library will arrange a loan.

OPERATED BY
MARTIN MARIETTA ENERGY SYSTEMS, INC.
FOR THE UNITED STATES
DEPARTMENT OF ENERGY

This report has been reproduced directly from the best available copy.

Available to DOE and DOE contractors from the Office of Scientific and Technical Information, P.O. Box 62, Oak Ridge, TN 37831; prices available from (615) 576-8401, FTS 626-8401.

Available to the public from the National Technical Information Service, U.S. Department of Commerce, 5285 Port Royal Rd., Springfield, VA 22161.
NTIS price codes—Printed Copy: A03 Microfiche: A01

This report was prepared as an account of work sponsored by an agency of the United States Government. Neither the United States Government nor any agency thereof, nor any of their employees, makes any warranty, express or implied, or assumes any legal liability or responsibility for the accuracy, completeness, or usefulness of any information, apparatus, product, or process disclosed, or represents that its use would not infringe privately owned rights. Reference herein to any specific commercial product, process, or service by trade name, trademark, manufacturer, or otherwise, does not necessarily constitute or imply its endorsement, recommendation, or favoring by the United States Government or any agency thereof. The views and opinions of authors expressed herein do not necessarily state or reflect those of the United States Government or any agency thereof.

ORNL/TM-11160

Engineering Physics and Mathematics Division

Shield Optimization Program, Part V: A Hydrodynamic Comparison Using HULL and PUFF-TFT for a One-Dimensional Aluminum Slab

M. S. Smith, T. J. Burns, and J. O. Johnson

DATE PUBLISHED — June 1989

Prepared by the
OAK RIDGE NATIONAL LABORATORY
Oak Ridge, Tennessee 37831
operated by
MARTIN MARIETTA ENERGY SYSTEMS, INC.
for the
U.S. DEPARTMENT OF ENERGY
under contract DE-AC05-84OR21400

MARTIN MARIETTA ENERGY SYSTEMS LIBRARIES

3 4456 0299808 6

CONTENTS

ABSTRACT vii
1. INTRODUCTION 1
1.1 BACKGROUND 1
1.2 PUFF–TFT 1
1.3 HULL 2
2. SOURCE SPECIFICATION 3
3. RESULTS AND DISCUSSION 4
3.1 TIME = 0.0 4
3.2 TIME = 0.1μsec. 4
3.3 TIME = 0.2μsec. 5
3.4 TIME = 0.3μsec. 5
3.5 TIME = 0.5μsec. 6
3.6 TIME = 1.0μsec. 6
4. CONCLUSIONS 7
5. ACKNOWLEDGMENTS 8
REFERENCES 25

LIST OF FIGURES

Figure		Page
1	Energy deposition as a function of depth	9
2	Density as a function of depth at 0.1μsec	10
3	Internal energy as a function of depth at 0.1μsec	11
4	Hydrostatic pressure versus depth at 0.1μsec	12
5	Density as a function of depth at 0.2μsec	13
6	Internal energy as a function of depth at 0.2μsec	14
7	Hydrostatic pressure versus depth at 0.2μsec	15
8	Density as a function of depth at 0.3μsec	16
9	Internal energy as a function of depth at 0.3μsec	17
10	Hydrostatic pressure versus depth at 0.3μsec	18
11	Density as a function of depth at 0.5μsec	19
12	Internal energy as a function of depth at 0.5μsec	20
13	Hydrostatic pressure versus depth at 0.5μsec	21
14	Density as a function of depth at 1.0μsec	22
15	Internal energy as a function of depth at 1.0μsec	23
16	Hydrostatic pressure versus depth at 1.0μsec	24

ABSTRACT

Results from the PUFF-TFT code were compared with those from HULL for a 1 dimensional aluminum slab subjected to X–rays from a 5 keV blackbody source. The source spectra was equivalent to a 1.5 Megaton thermonuclear device detonated at a distance of 10 km. Code predictions of density, internal energy, fracture locations, and axial stress were examined. With the exception of the magnitude of the axial stress, results from both codes were in agreement as to the characteristics of the material response.

1. INTRODUCTION

This report discusses the results of a comparative study between two hydrodynamic computer codes. The purpose of the study was to identify the similarities and differences in the predicted responses between the PUFF-TFT[1] and HULL[2] codes. The HULL code was used to validate the PUFF–TFT results; HULL has been used by this group for penetration mechanics studies for several years. Although the two codes are dissimilar in their approach to solving hydrodynamics problems, both are capable of characterizing the effect of incident X–rays upon a medium.

1.1 BACKGROUND

Results for this study were generated using a hydrodynamic computer code, or hydrocode. Hydrocodes solve the set of differential equations arising from the conservation of mass, momentum, and energy, coupled with an equation of state and a constitutive relation. The equation of state relates the materials density (or volume) and internal energy (or temperature) with pressure. A constitutive relation describes the particular nature of the material by relating the stress in the material with the amount of distortion (strain) required to produce this stress. The constitutive relation may include strain rate effects, work hardening, thermal heating/softening, etc.

The formulation of the differential equations follow either Eulerian or Lagrangian descriptions. The Eulerian description is a spatial description; the Lagrangian is a material description. In an Eulerian framework, all grid points, and consequently cell boundaries, remain fixed with time. Mass, momentum, and energy flow across cell boundaries. In a Lagrangian description, the grid points are attached to the material and move with the material. In this formulation, mass within a cell is invariant, but the volume of the cell may change with time because of expansion or compression of the material.

1.2 PUFF–TFT

The PUFF-TFT code was used to assess the hydrodynamic response from incident X–rays on a medium. The coupling of the TFT (Thin Film Transport) module with the PUFF74 code has been performed by Ktech Corporation. The TFT package accounts for the effects of dose enhancement due to the transport of secondary particles with ranges comparable to the thickness of the thin material layers and thermal conduction between thin material layers. These two modifications (among others) more accurately portray the degree of energy sharing between thin layers, thereby modifying the expected energy depositions based on normal X–ray interactions and possibly altering the anticipated thermo–mechanical response of the medium.

The PUFF74 code,[3] originally developed in the mid–sixties, has undergone a number of revisions to become a flexible material response code that includes the effects of material strength, porosity, and fracture for both homogeneous and

composite materials. The code calculates stress wave formation and propagation by numerical integration of the conservation equations in a one–dimensional Lagrangian coordinate system. In addition to the hydrodynamic equation of state, which is required for all materials, the code contains an elastic–plastic model for strength effects, a P–α porosity model for treating irreversible compaction, and four models for treating strain–rate dependent or dispersive effects.

1.3 HULL

The HULL hydrodynamic code is designed to solve the time–dependent equations of continuum mechanics: conservation of mass, momentum, and energy. These equations may be solved using an Eulerian formulation (fixed mesh cell with moving materials) or a Lagrangian formulation wherein material transfer between cells is prohibited, but the mesh itself can distort. Additionally, a problem can consist of both Eulerian and Lagrangian regions.

Geometry options included in HULL comprise both two–dimensional (R–Z and X–Y) and three–dimensional (X–Y–Z). HULL is currently programmed for 15 types of constitutive relations such as Gamma–Law gas, Mie–Gruniesion, etc. It provides capabalility for the inclusion of high explosives as part of the problem via the inclusion of constitutive relations for both the explosives themselves as well as the detonation products. The material property library associated with the constitutive relations contains a significant number of materials including a number of metals, water, sand, concrete, etc.

The HULL hydrocode can optionally account for material failure in a number of ways ranging from simple stress or strain criteria to complex failure surfaces. Additionally, depending on the particular equation of state, the effects of material melting and vaporization can be included in the calculation.

2. SOURCE SPECIFICATION

A nuclear detonation will heat the device and surrounding material to tens of millions of degrees Kelvin. Due to this large temperature, blackbody radiation will occur in the form of X-ray radiation. Approximately 75% of the total energy emitted during a detonation will appear in this form of emission[4].

The differential energy distribution (X-rays/unit energy) associated with blackbody X-rays can be written

$$\frac{dN(E,kt)}{dE} = \frac{CE^2}{e^{E/kT} - 1}$$

where N is the number of X-rays with energy E about dE, kT is the temperature of the emitting object, and C is a normalization factor[5]. As the temperature of the blackbody radiator increases, the emission spectrum hardens. For the purpose of this study, a 1.5 Megaton thermonuclear device was chosen with a temperature (kT) equal to 5 keV. The device was assumed to detonate 10 kilometers from the aluminum slab yielding an X-ray flux of 1.7332×10^{17} X-rays/cm^2 incident on the slab. The average energy of an emitted X-ray for this device temperature is 13.5 keV. This corresponds to a surface loading of 89.56 cal/cm^2.

Calculations were performed with the Electron Gamma-Ray Shower Code EGS4[6] to determine the energy deposition as a function of depth in an aluminum slab of thickness 0.16 cm. The preliminary results showed energy deposition rates large enough to damage the slab if the thermonuclear device was sufficiently large enough and/or close enough to the spacecraft. The energy deposition profiles obtained from the EGS4 calculations were used in the HULL hydrodynamics code to calculate the physical damage (melting, vaporization, blow-off, etc.) to the slab.

The EGS4 calculation was performed using a variable mesh. In particular, a 0.001 cm thick interval was used in the first 0.02 cm, a 0.002 cm thick interval was used in the next 0.02 cm, a 0.005 cm thick interval was used in the next 0.04 cm, and a 0.01 cm thick interval was used in the remainding 0.08 cm. The EGS4 calculation analyzed 50,000 source particles incident on the aluminum slab.

3. RESULTS AND DISCUSSION

Two hydrodynamic computer codes, HULL and PUFF-TFT, have been used to assess the thermo–mechanical response of an aluminum slab from incident X–rays characteristic of an exo-atmospheric nuclear detonation. A blackbody spectrum at 5 keV was normalized to yield a surface loading of approximately 90 cal/cm^2. This corresponds to a 1.5 Megaton detonation at a distance of 10 kilometers, assuming 75% of the energy is in the form of X–rays. The aluminum target was 0.16 cm thick, with a density of 2.71 g/cm^3. In this analysis, the PUFF–TFT code employed vacuum boundary conditions while the HULL code used low density air to simulate vacuum boundary conditions. Material properties were obtained from Rice[7] (p. 16) and Childs[8] (p.21).

For a detailed comparison of the two codes capabilities, an examination of the density, internal energy, axial stress, mass fractions of vapor, liquid, and solid phases, and fracture locations at six time intervals: 0.1, 0.2, 0.3, 0.5, and 1.0 μsecond was performed. In addition, the initial energy deposition was also examined.

3.1 TIME = 0.0

The energy deposition calculations are performed for both codes prior to the initial time step. HULL uses the energy deposited from the EGS4 code as an impulse. For the HULL code, the aluminum was subdivided into 64 uniform spatial grid points. PUFF computes the energy deposition from the blackbody spectrum and surface loading and allocates the energy over a specified time frame. PUFF employed an automatic zoning procedure that generated about twice as many mesh cells (nonuniform) as was used in the HULL calculations. For this problem, all of the energy was deposited within 1 nanosecond. Figure 1 shows the energy deposition as a function of depth for each code. The calculated energy deposition as a function of depth is essentially identical for the two codes. The calculated error for EGS is within $\pm 10\%$ ($\pm 1\sigma$).

From the energy deposition, the PUFF code flags those cells that have vaporized or melted. Cell masses are summed and mass fractions computed for each phase. A rough estimate of the mass fractions in each phase can be made for HULL from the initial internal energy. Table 1 lists the calculated mass fraction by phase for each code at time = 0.0. If it is assumed the two phase regions in the HULL calculations are equally proportioned between the solid/liquid and liquid/vapor phases, excellent agreement is obtained with PUFF *i.e.*, for HULL, half of the two phase liquid/solid region can be added to the liquid only portion to yield $\approx$ 22%, as compared to 21.5% from the PUFF code.

3.2 TIME = 0.1μsec.

Figures 2 through 4 compare density, internal energy, and axial stress as a function of depth. Included with the plot of density are vertical dashed lines denoting fracture locations as predicted by PUFF. Similarly, phase transitions

Table 1.
Approximate Mass Fractions by Phase

	PUFF	HULL
Vapor	2.5%	
2ϕ		3%
Liquid	21.5%	14%
2ϕ		16%
Solid	76.0%	67%

are marked on the plot of internal energy. These conventions will be continued throughout this analysis.

A close examination of Figure 2 reveals several interesting features. First it is noted that the ablation wave front from PUFF is much greater than that from HULL. This is not surprising due to the difference in boundary conditions, *i.e.*, vacuum vs. air. Both codes are in agreement as to the solid density, although PUFF predicts a small increase in density at the location of peak axial stress (see Figure 4). Both codes also predict a density spike which occurs for PUFF at the vapor/liquid interface. This liquid wave front is beginning to separate from the remaining material according to the HULL code. The PUFF code shows early fracture locations at the liquid/solid interface.

The plots of internal energy (Figure 3) are in good agreement. Here also PUFF calculates a small increase in internal energy at the peak axial stress location. The rapid expansion of the ablated material is again evident from the PUFF results. An attempt was made to correct one of the many differences in the two codes: HULL includes an ambient component in its internal energy, *i.e.*, at 300 K, the internal energy of aluminum is about 60 cal/g. This was added to the PUFF value for this comparison. Figure 4 compares axial stress. Although both codes agree on the location of the peak stress, there is a considerable difference in the magnitude. This difference cannot be explained at this time, although efforts are underway to achieve this.

3.3 TIME = 0.2μsec.

Figures 5 through 7 compare density, internal energy, and axial stress at 0.2μsec. The HULL code shows a second separation in the liquid region (Figure 5) and a small drop in density at ≈ 0.08 cm which will become a fracture point. PUFF has also predicted a fracture at this location. The internal energy is in good agreement (Figure 6) and the axial stress is again off in magnitude but exact in location (Figure 7).

3.4 TIME = 0.3μsec.

By 0.3μseconds, PUFF predicts a large number of material fractures and HULL is showing several regions of reduced density in the solid (Figure 8). These regions of reduced density are the Eulerian equivalent of fracture locations. In the liquid

region, HULL is indicating some strong density oscillations, that may correspond to waves of material being ablated. The leading liquid wave front is still in good agreement at this point. This fracture has now shown up in the plot of internal energy (Figure 9). PUFF's calculation of internal energy is somewhat larger than the HULL value and this also, needs to be reconciled. The axial stress wave has been reflected at this point, and there is little agreement in magnitude or form (Figure 10). The yield stress was set at 20 kbar, and this has effectively limited the magnitudes of the axial stress oscillations.

3.5 TIME = 0.5μsec.

Conceptually, there is little change at the later times. The HULL density waves in the liquid region are more numerous and the solid fracture lines more pronounced (Figure 11). The difference in internal energy has grown, particularly in the liquid phase (Figure 12). The overall magnitude of the axial stress waves are close, but there is no association in position (Figure 13).

3.6 TIME = 1.0μsec.

At this final time value, there is still good agreement in the density (Figure 14). Both codes are consistent in the location and magnitude of the leading liquid wave front and PUFF is showing some oscillations in the liquid region. There is strong separation in both codes at the liquid/solid interface and further spallation in the interior of the solid. The HULL solid fracture points have shown up in the internal energy plot (Figure 15), but there is even less agreement in magnitude. PUFF predicts a primary and secondary stress (compression) pulse, whereas there appears to be some form of chaotic behavior in the HULL results (Figure 16).

4. CONCLUSIONS

Two computer codes were used to calculate the thermo-mechanical response of a 1D aluminum target to high levels of incident X–rays. The X–ray spectra was similar to that from a 1.5 Megaton thermonuclear device detonated at a distance of 10 km. The objective was to determine the calculational effectiveness of the PUFF-TFT hydrodynamics module and to gain hands-on experience with the code.

Both computer codes calculated extreme damage levels in the aluminum slab. Although there was considerable disagreement in the magnitude of the axial stress before the compressive wave reflected off the back surface and differences in shape after reflection, the end result for both codes was markedly similar. Density as a function of depth, fracture locations and times, and mass fractions were all equivalent. The internal energy compared well at earlier times, but less favorably at later times. Some differences are to be expected, but the prediction of the magnitude of the axial stress needs to be more thoroughly investigated. It is not known at this time which code is correct; perhaps the "true" value lies somewhere between the two calculated values. Overall, results from the PUFF code were in reasonable agreement with those from the more complex HULL model, and were obtained at a much lower cost.

5. ACKNOWLEDGMENTS

The authors wish to thank Mrs. Dawn C. Human for her significant efforts in typing this manuscript and for her assistance throughout this program.

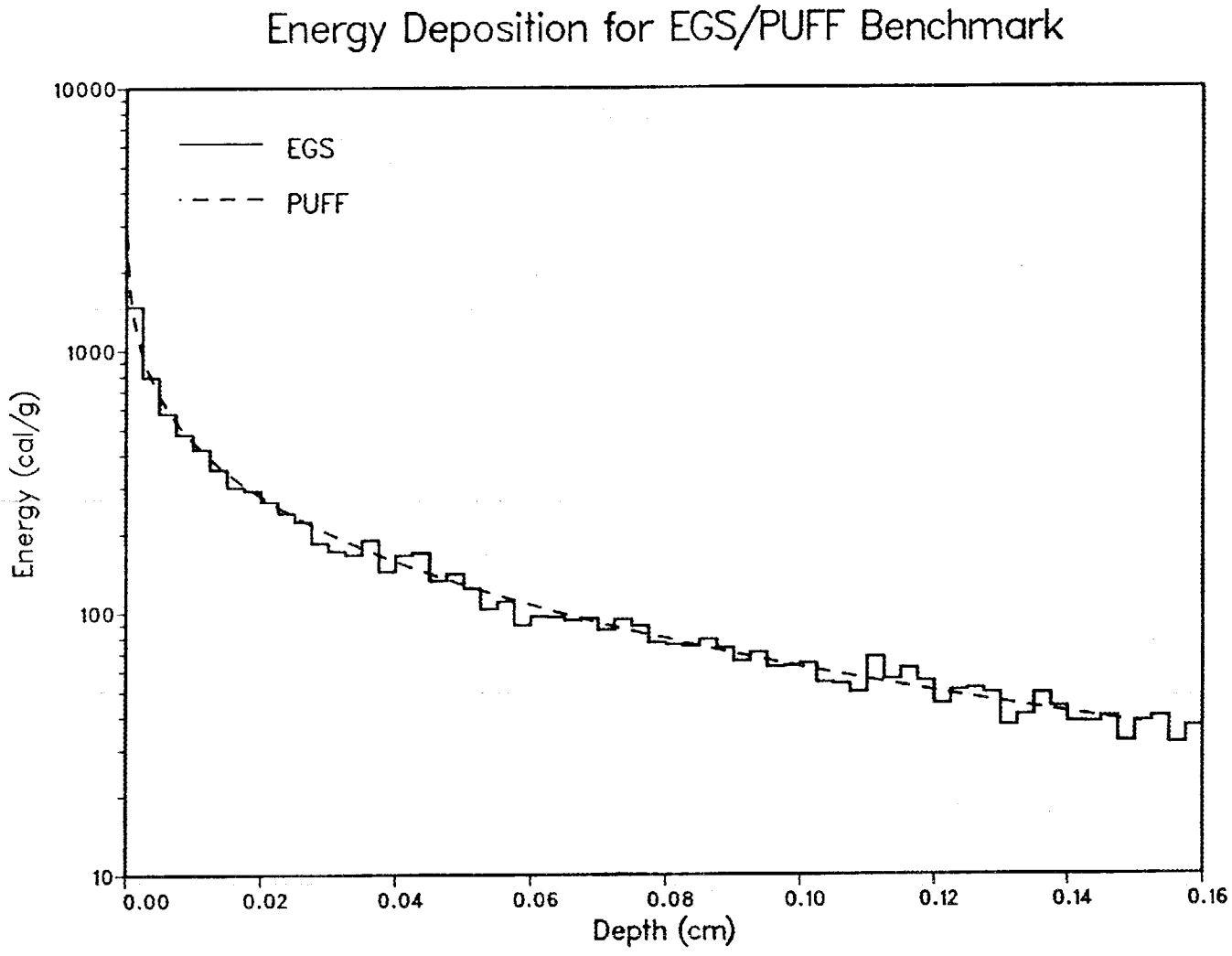

Figure 1. Energy deposition as a function of depth.

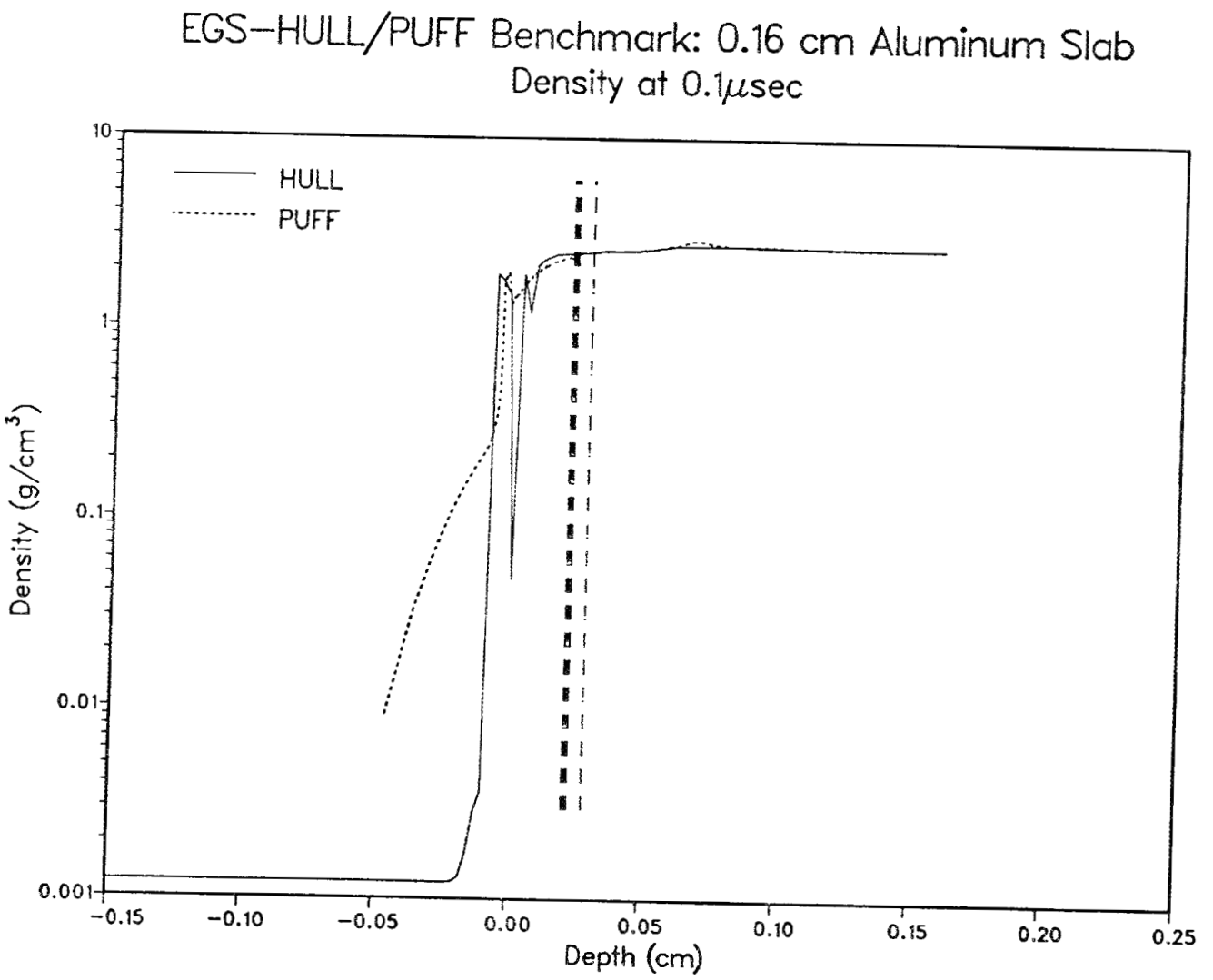

Figure 2. Density as a function of depth at 0.1μsec.
Vertical dashed lines denote fracture locations.

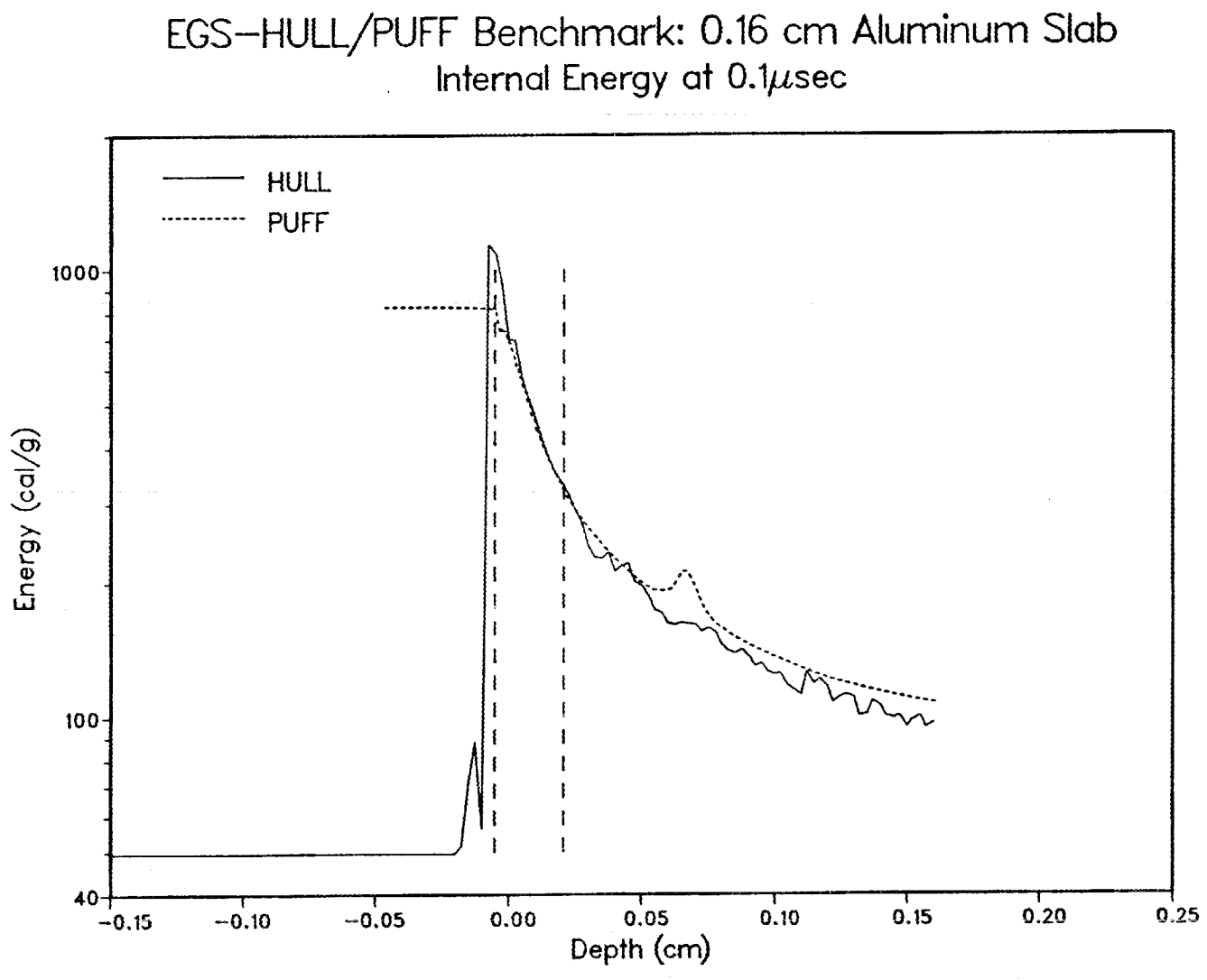

Figure 3. Internal energy as a function of depth at 0.1μsec. Vertical dashed lines denote phase transitions.

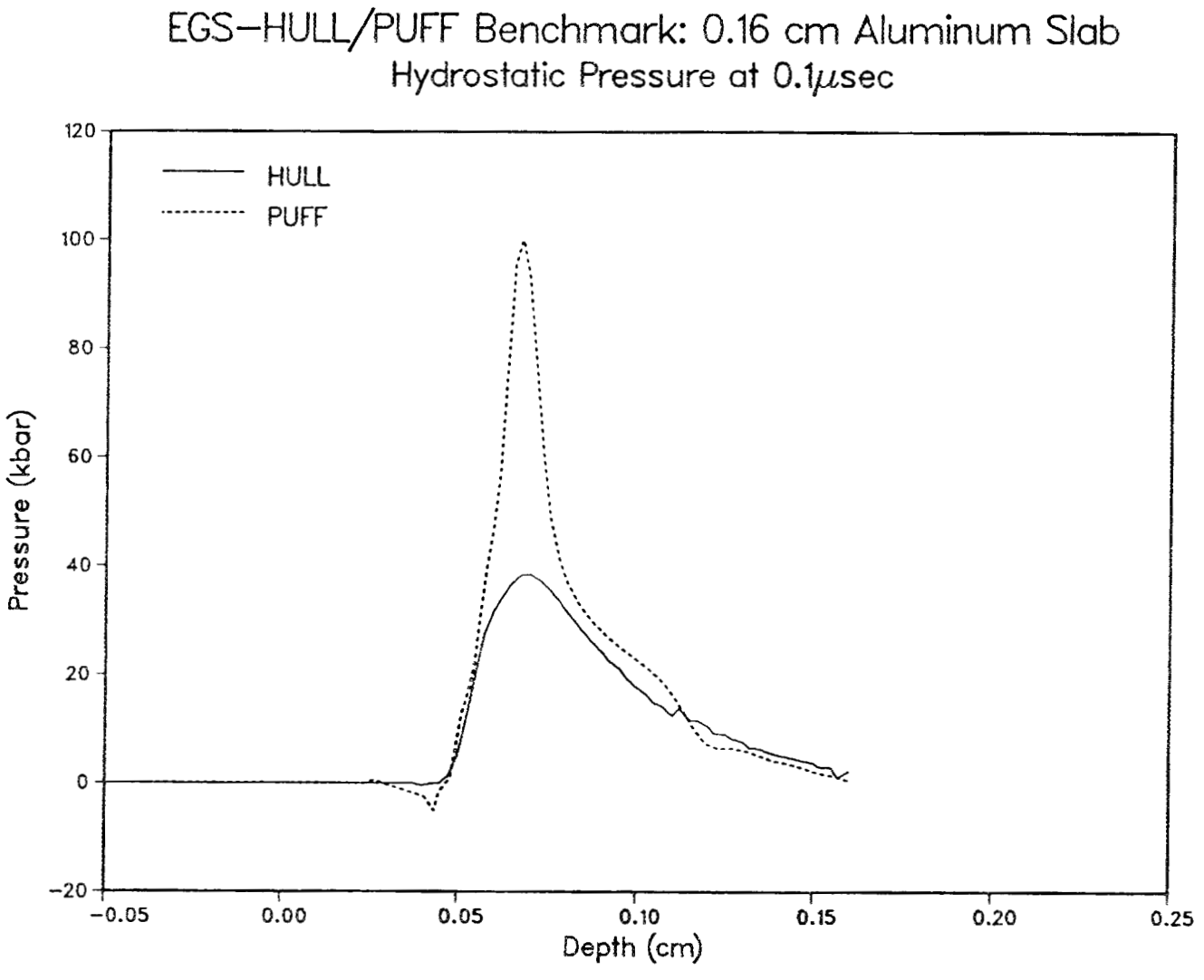

Figure 4. Hydrostatic pressure versus depth at 0.1μsec.

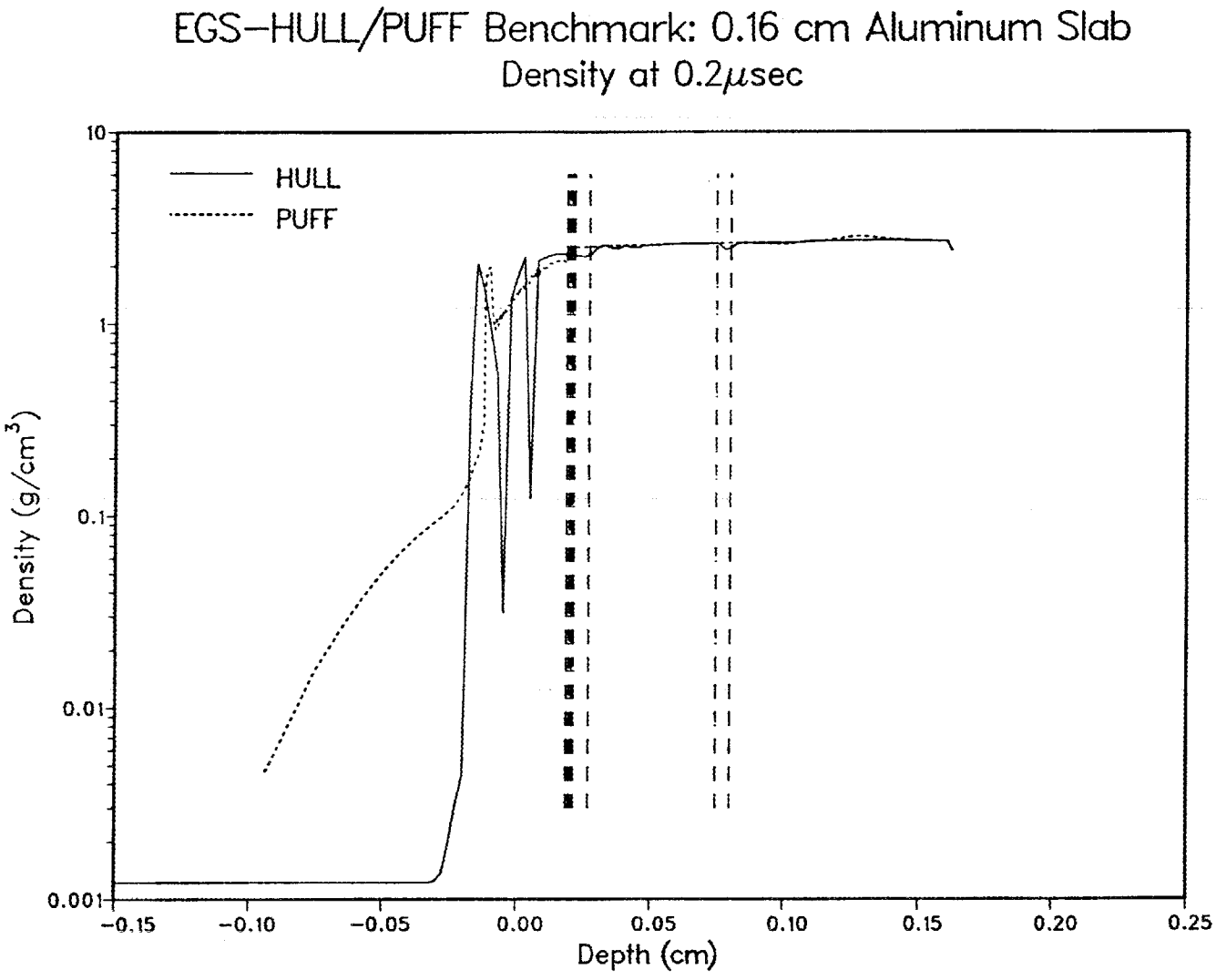

Figure 5. Density as a function of depth at 0.2μsec.
Vertical dashed lines denote fracture locations.

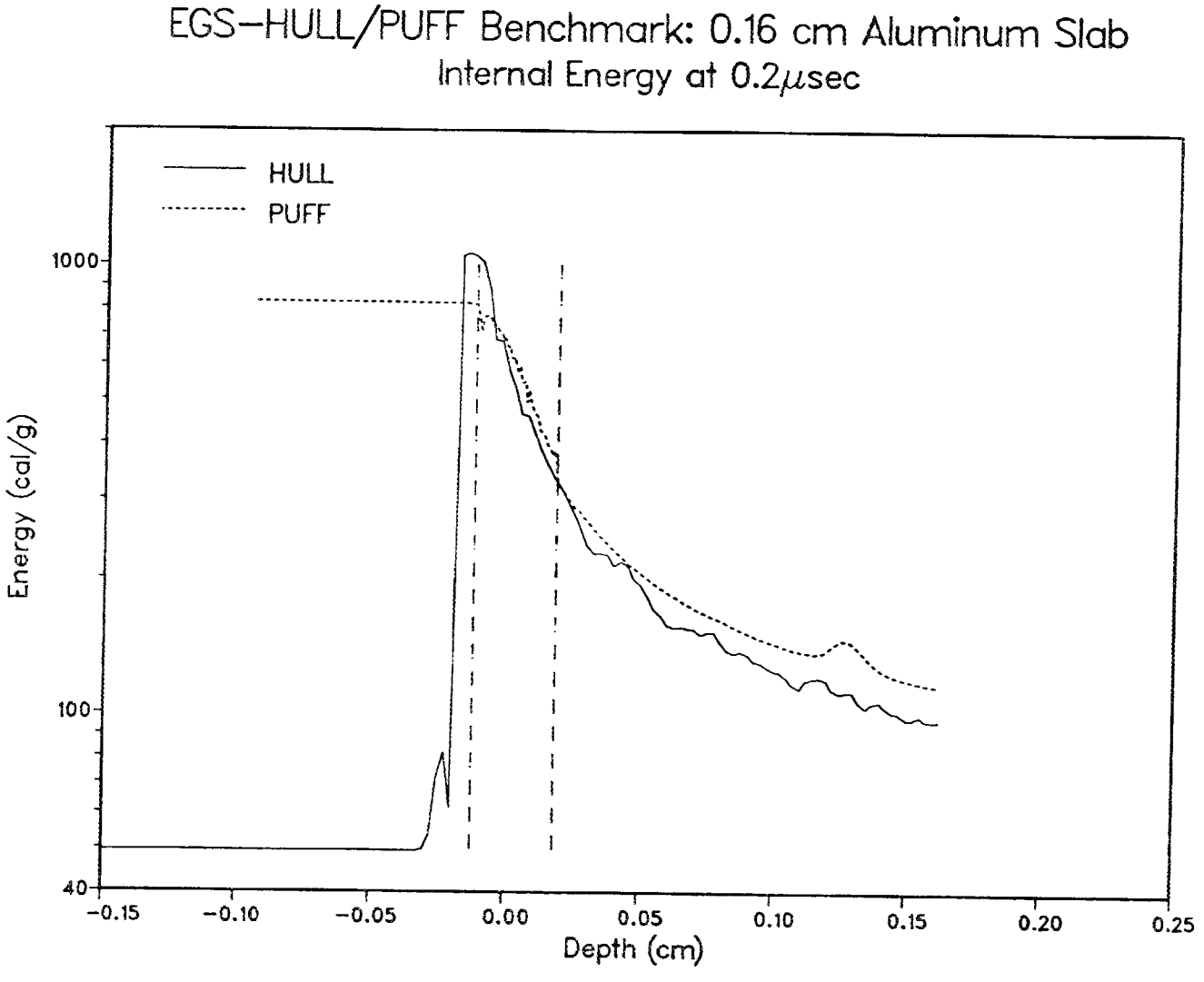

Figure 6. Internal energy as a function of depth at 0.2μsec. Vertical dashed lines denote phase transitions.

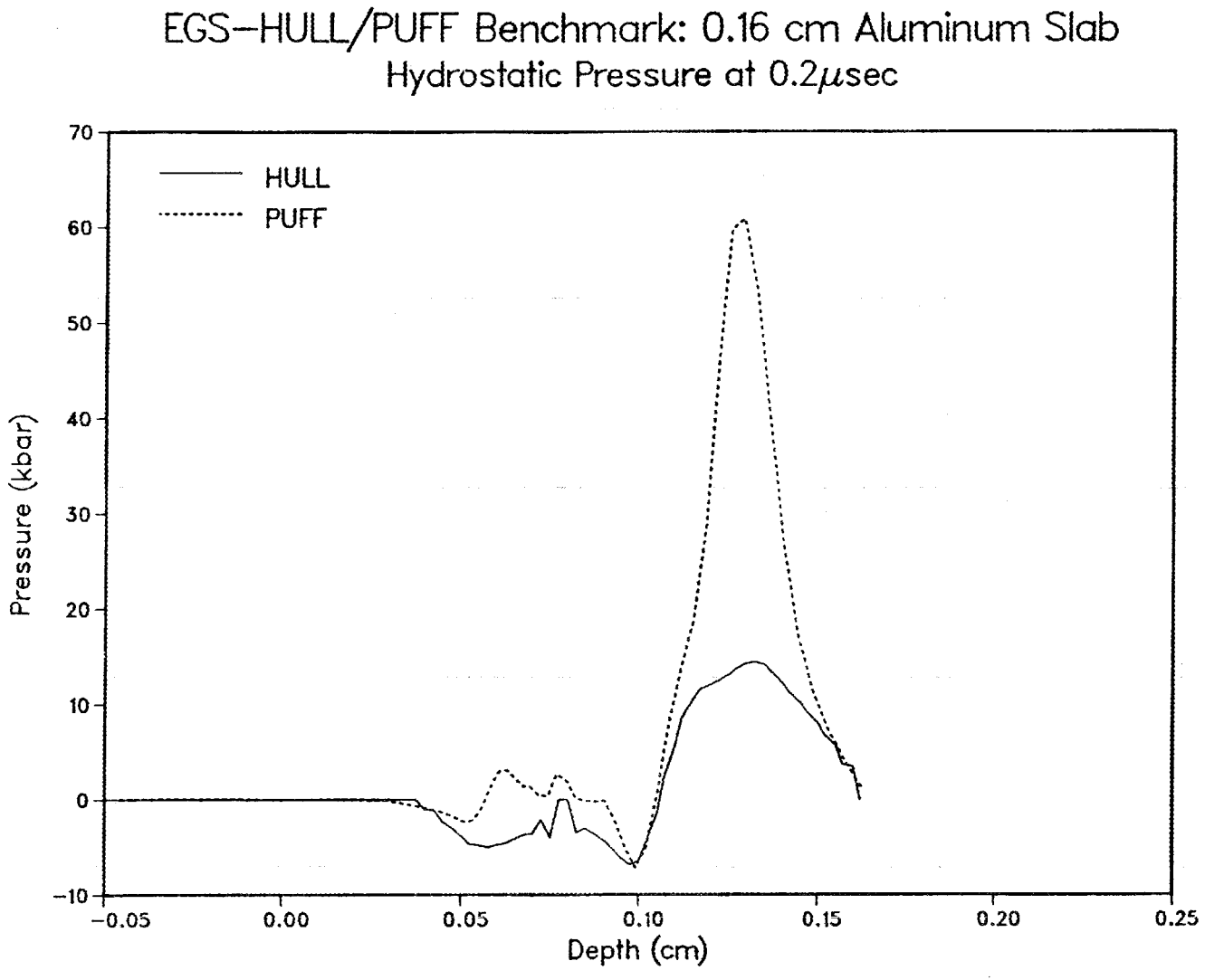

Figure 7. Hydrostatic pressure versus depth at 0.2μsec.

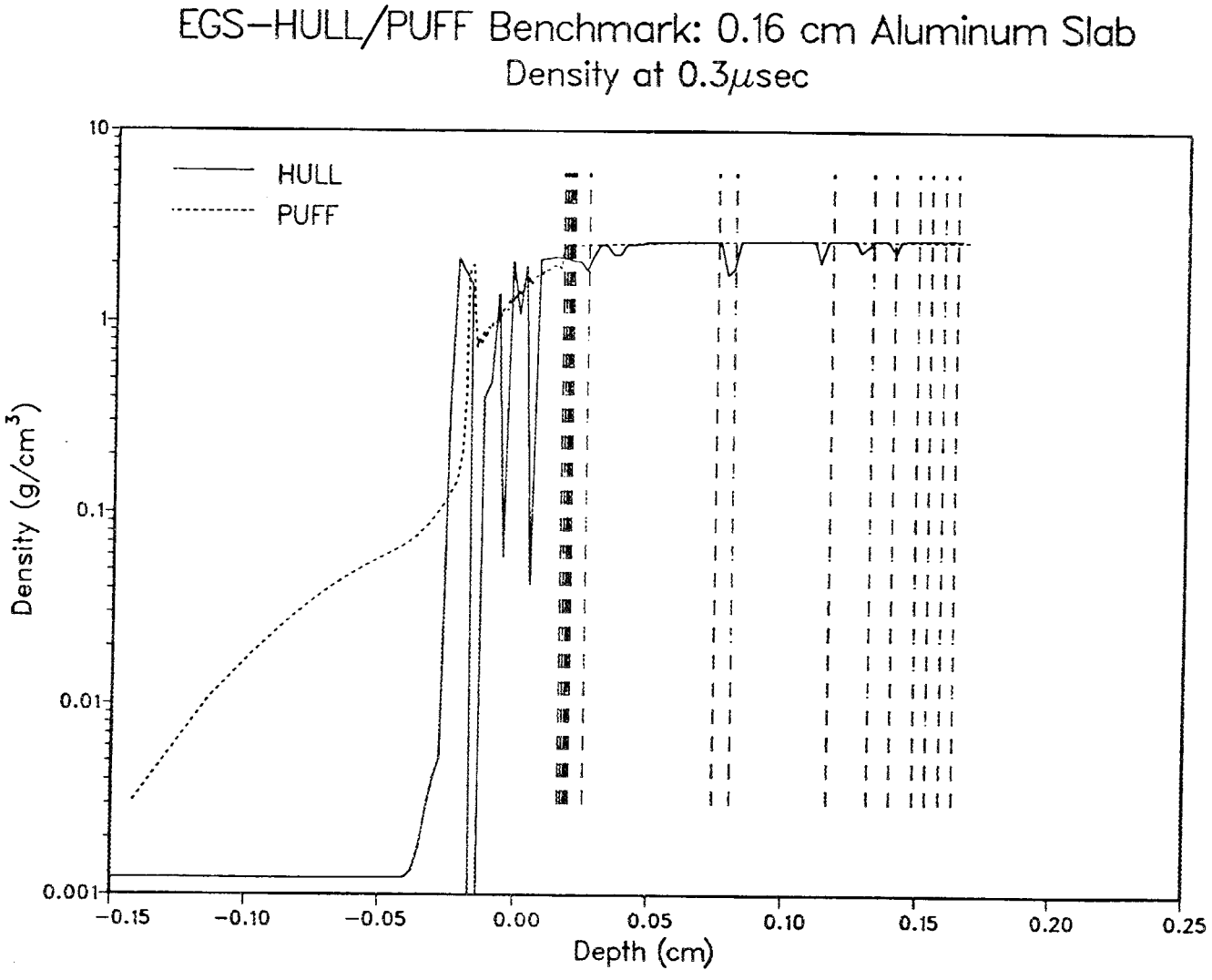

Figure 8. Density as a function of depth at 0.3μsec.
Vertical dashed lines denote fracture locations.

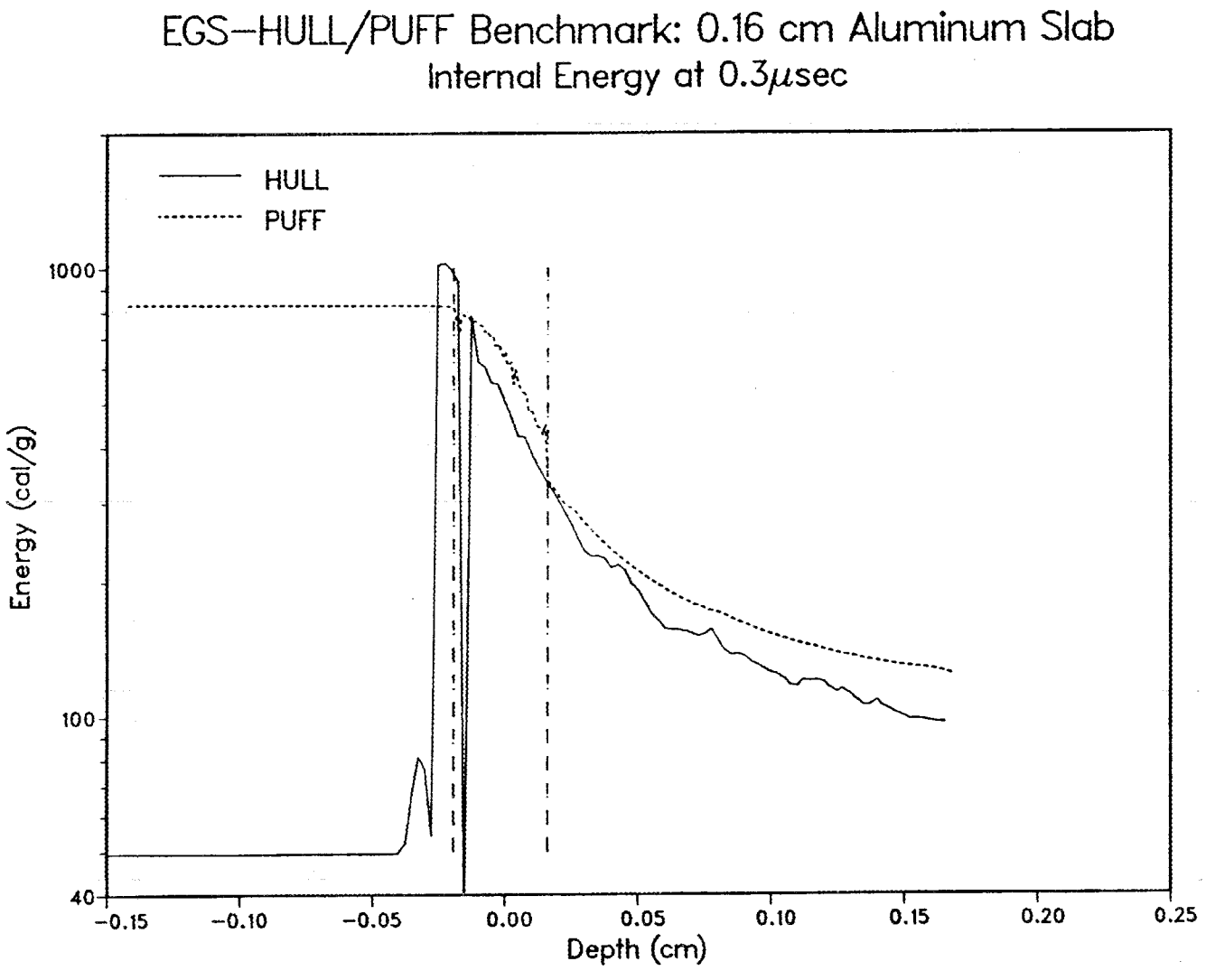

Figure 9. Internal energy as a function of depth at 0.3μsec. Vertical dashed lines denote phase transitions.

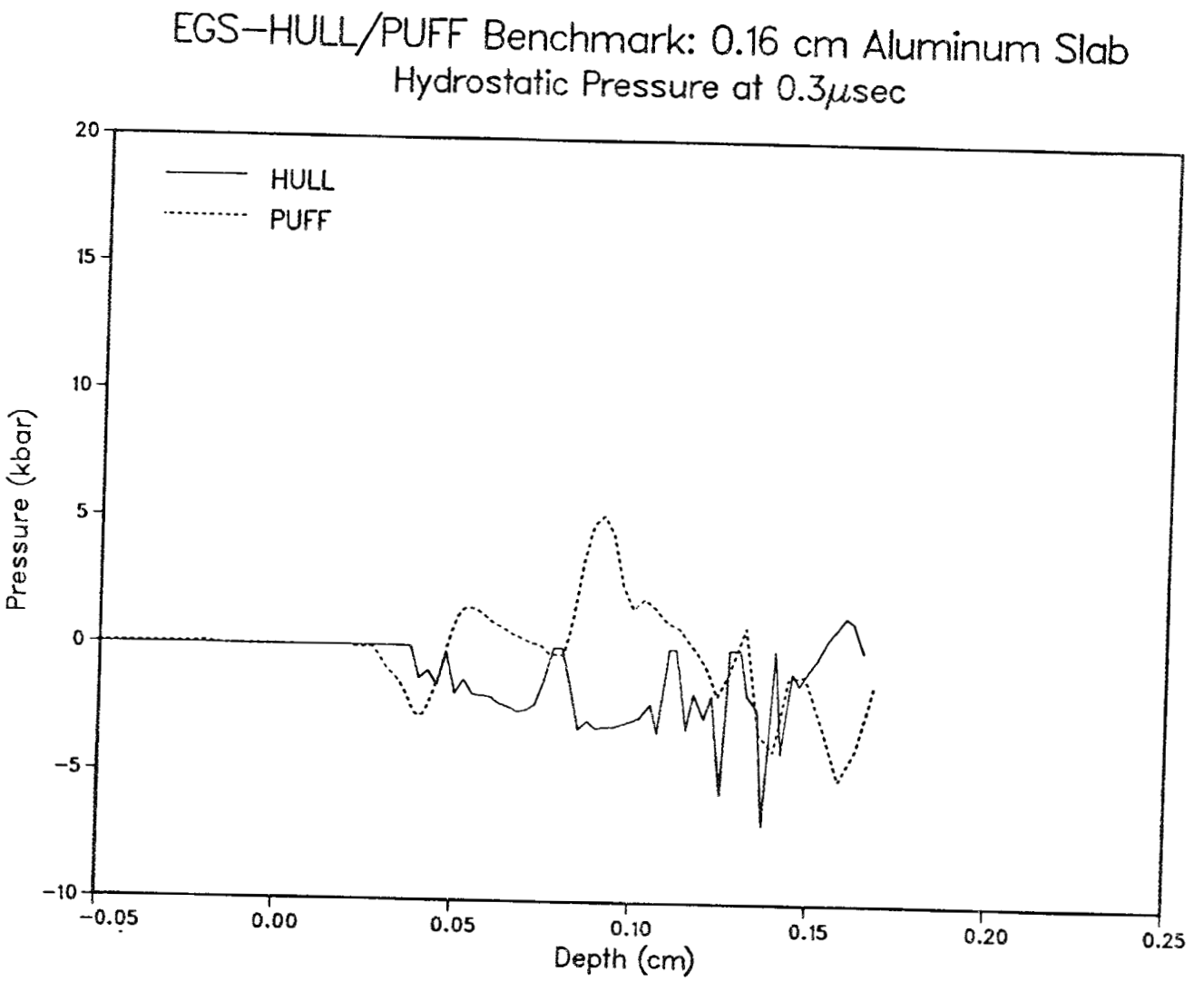

Figure 10. Hydrostatic pressure versus depth at 0.3μsec.

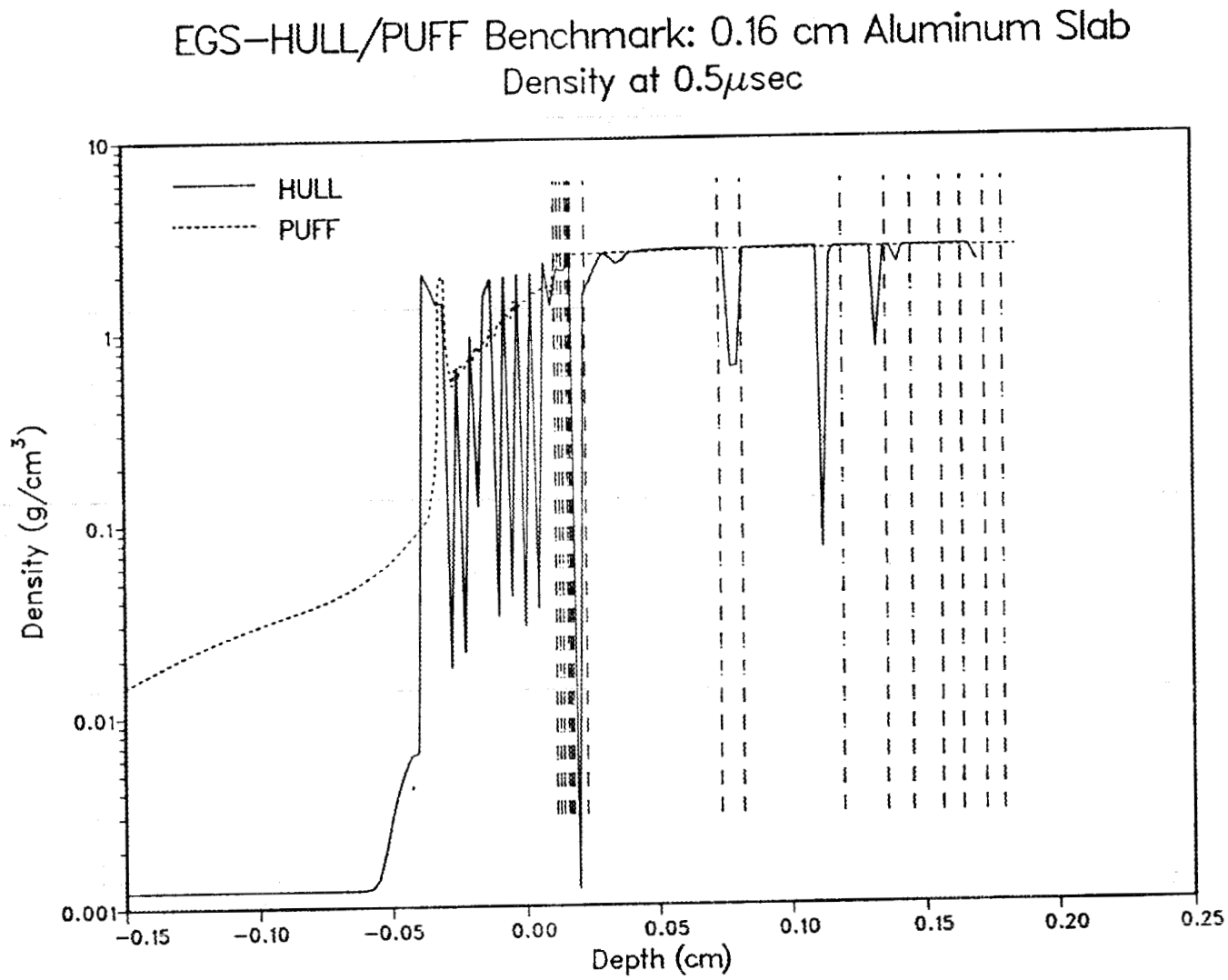

Figure 11. Density as a function of depth at 0.5μsec.
Vertical dashed lines denote fracture locations.

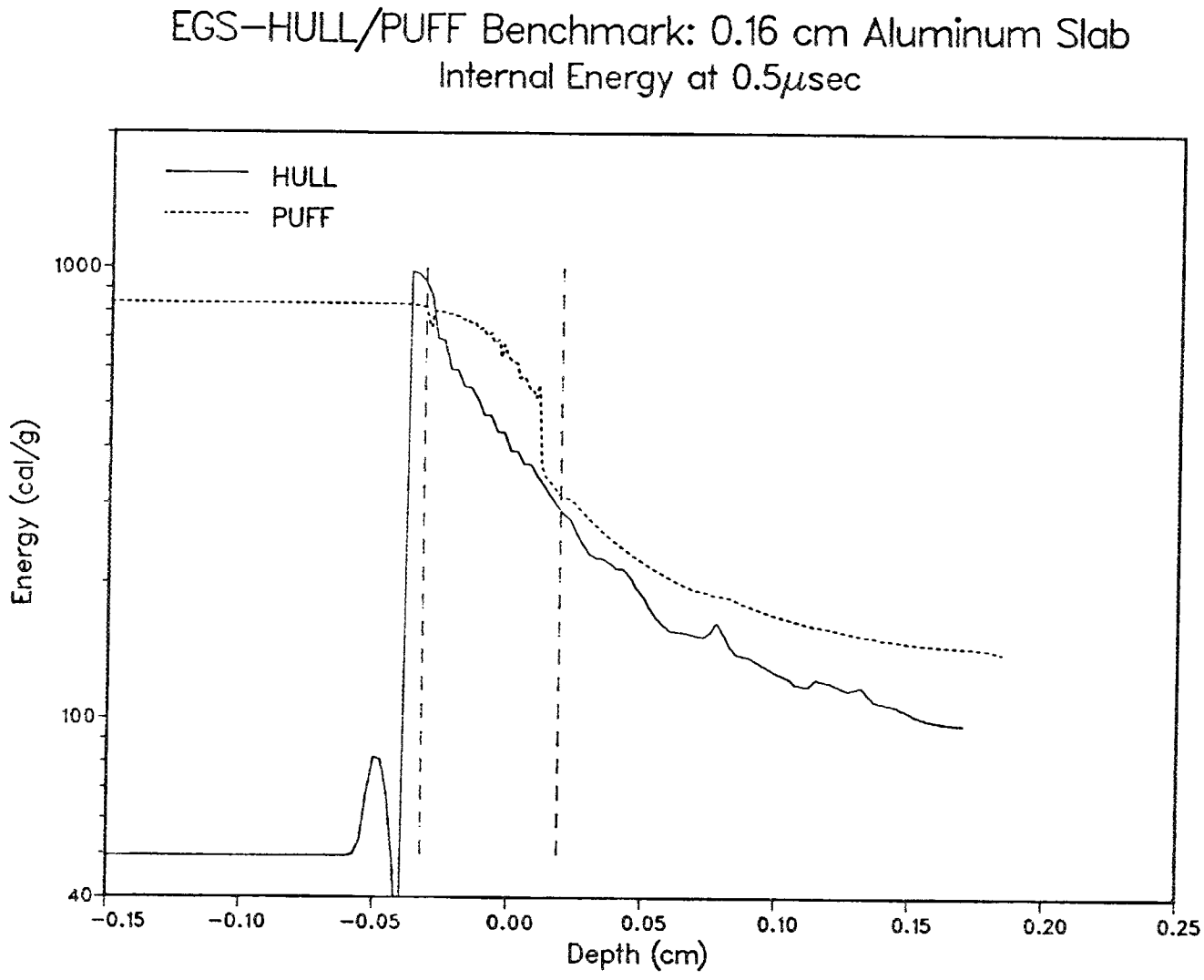

Figure 12. Internal energy as a function of depth at 0.5μsec. Vertical dashed lines denote phase transitions.

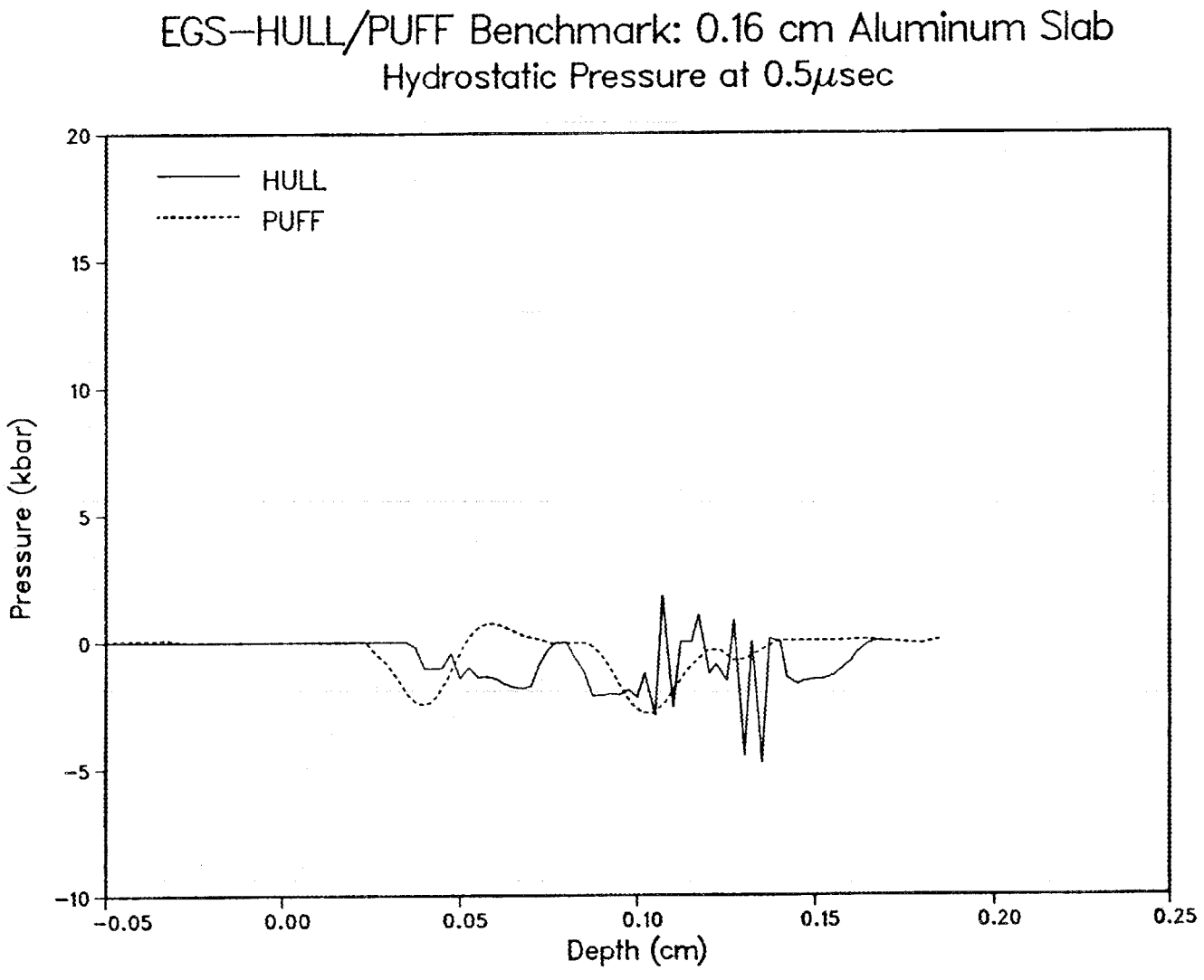

Figure 13. Hydrostatic pressure versus depth at 0.5μsec.

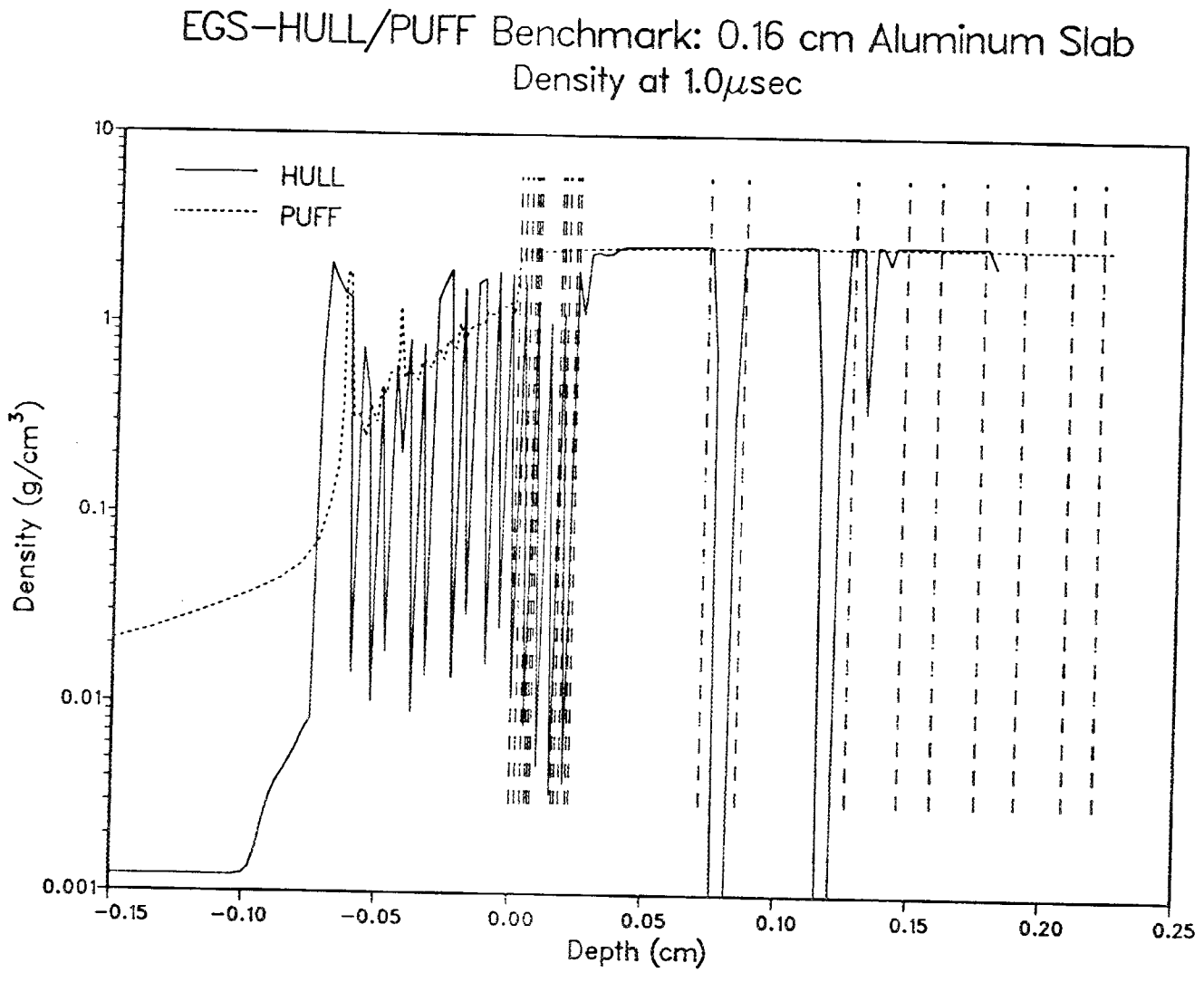

Figure 14. Density as a function of depth at 1.0μsec.
Vertical dashed lines denote fracture locations.

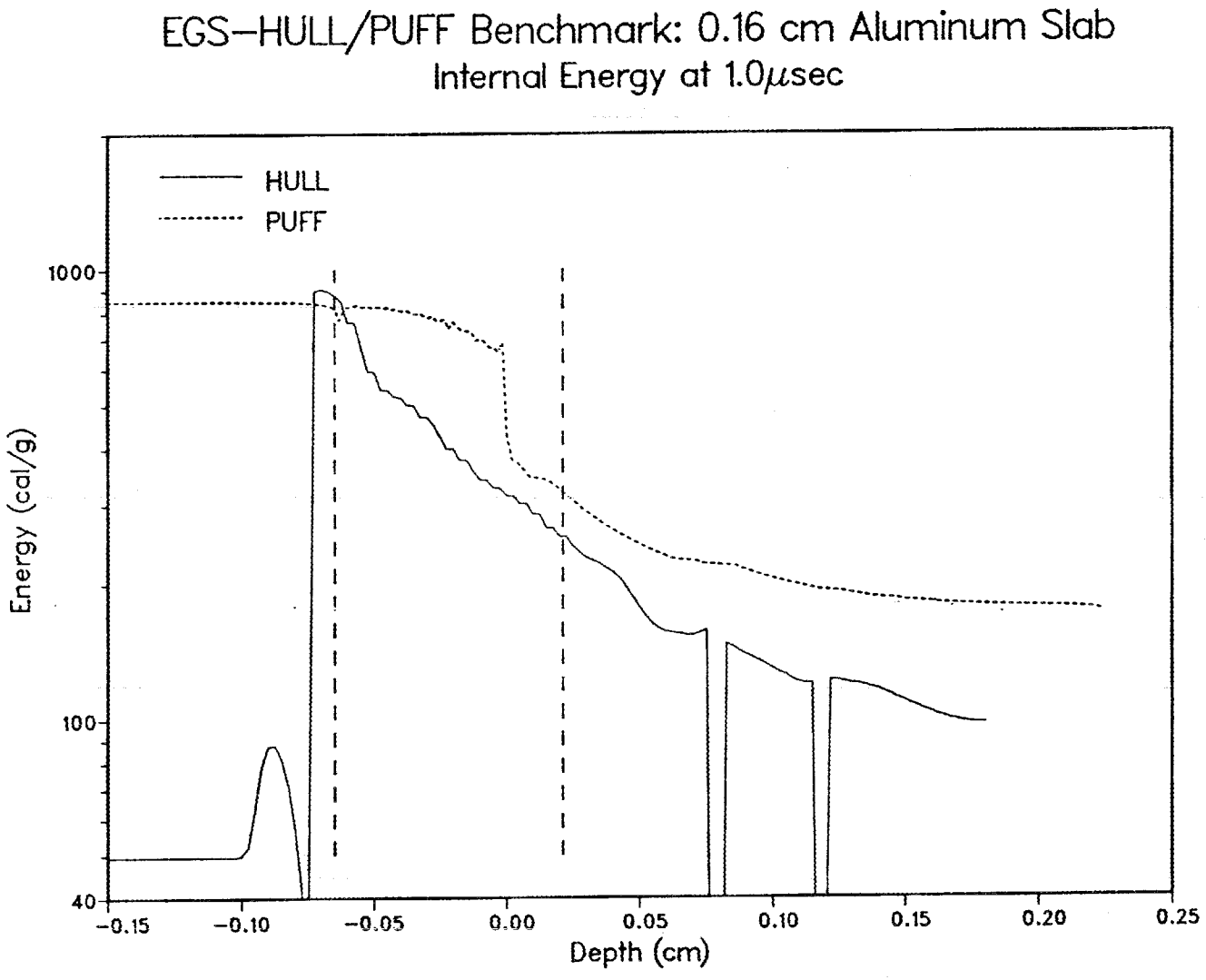

Figure 15. Internal energy as a function of depth at 1.0μsec. Vertical dashed lines denote phase transitions.

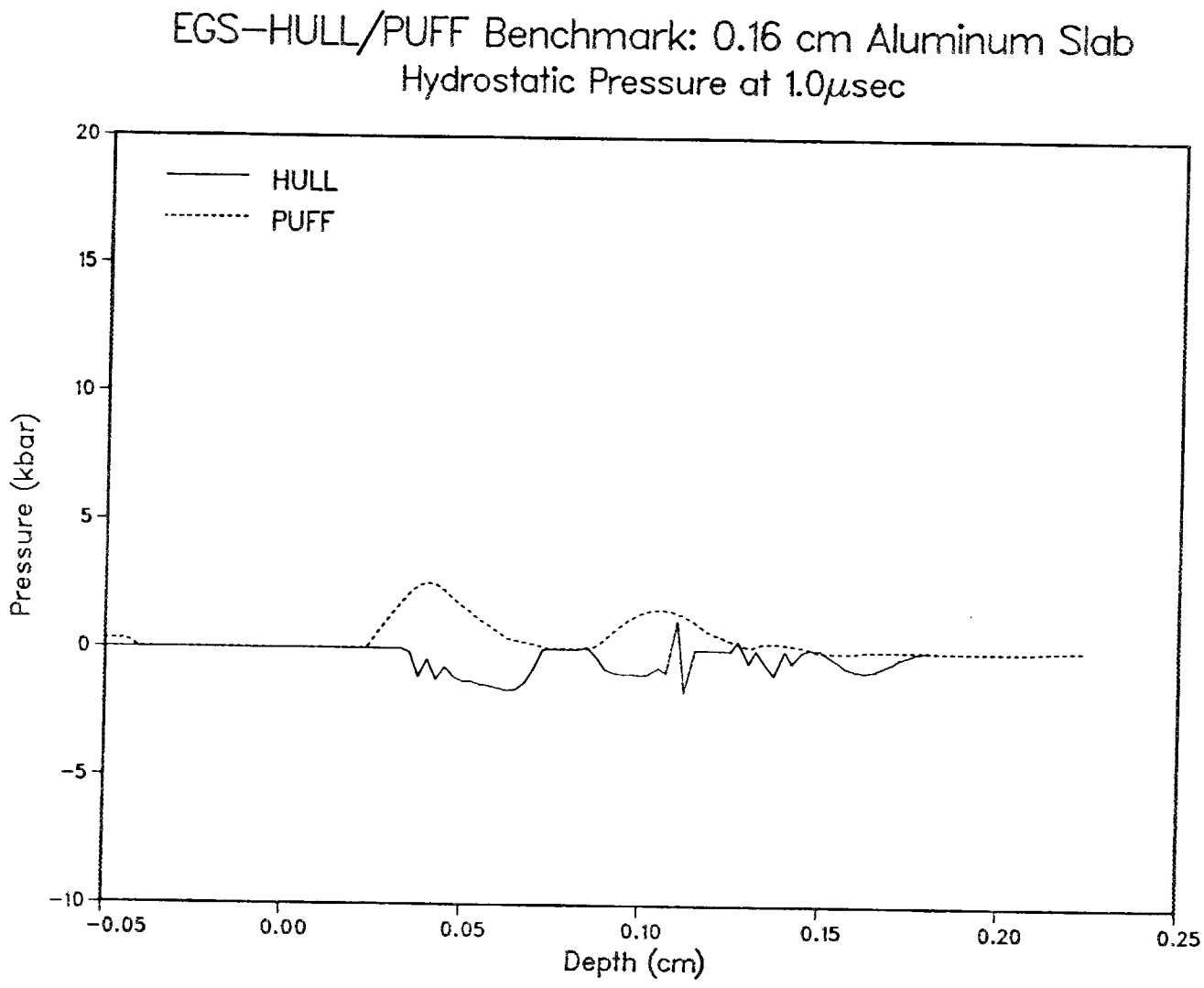

Figure 16. Hydrostatic pressure versus depth at 1.0μsec.

REFERENCES

1. A.J. Watts, C. Breen, S. Sauer, and F. Smith, "Thin Film Transport (PUFF–TFT) Computer Code Development," AFWL–TR–88–66, Parts 1 and 2, Air Force Weapons Laboratory, Kirtland AFB, NM, June 1988.
2. D. A. Matuska, and J. J. Osborn, "The HULL Code System," Orlando Technology, Inc., Shalimar Fla. (1983).
3. R. Cecil, C.D. Newlander, and R.T. Scannon, "PUFF74 – A Material Response Computer Code," AFWL–TR–76–43, Volumes I and II, Air Force Weapons Laboratory, Kirtland AFB, NM, January 1977.
4. MAJ R. Leong, 1LT D. Lahti, 1LT K. Murphy, 1LT S. Rieco, 1LT R. Zacharko, "AFWL Exoatmospheric Nuclear Radiation Environment Prediction and Shielding Codes Applicable to the Strategic Defense Initiative (SDI)," Draft Report, Air Force Weapons Laboratory, Kirtland Air Force Base, New Mexico, May 1986.
5. R. Siegel and J. R. Howell, *Thermal Radiation Heat Transfer*, Mcgraw-Hill, Inc., 1972.
6. W. R. Nelson, H. Hirayama, and D. W. O. Rogers, "The EGS4 Code System - A Monte Carlo Simulation of the Coupled Transport of Electrons and Photons," Stanford Linear Accelerator Center, Stanford, CA, SLAC-265, (1985).
7. M. H. Rice, "PUFF74 EOS Compilation," AFWL–TR–80–21, Air Force Weapons Laboratory, Kirtland AFB, NM, August 1980.
8. W. H. Childs, "Thermophysical Properties of Selected Space–Related Materials," TOR–0081(6435–02)–1, Volume I, Aerospace Corporation, Los Angeles, CA, February 1981.

INTERNAL DISTRIBUTION

1. R. G. Alsmiller, Jr.
2. B. R. Appleton
3. D. E. Bartine
4. J. M. Barnes
5–9. T. J. Burns
10. R. M. Davis
11. J. B. Dooley
12. J. D. Drischler
13. T. A. Gabriel
14. E. B. Harris
15. D. T. Ingersoll
16–20. J. O. Johnson
21. F. C. Maienschein
22. S. McNeany
23. J. R. McNeely
24. J. R. Merriman
25. W. L. Roberts
26. R. W. Roussin
27. R. T. Santoro
28–32. M. S. Smith
33. D. G. Thomas
34. R. C. Ward
35. C. R. Weisbin
36. J. M. Williams
37. EPMD Reports Office
38–39. Laboratory Records Department
40. Laboratory Records, ORNL–RC
41. Document Reference Section
42. Central Research Library
43. ORNL Patent Section

EXTERNAL DISTRIBUTION

44. Dr. Charles Aeby, AFWL/NTC, Air Force Weapons Laboratory, Kirtland Air Force Base, New Mexico 87117-6008
45. Lt Dale Atkinson, AFWL/NTCA, Air Force Weapons Laboratory, Kirtland Air Force Base, New Mexico 87117-6008
46. Richard Bradshaw, U.S. Army Strategic Defense Command, 106 Wynn Drive, Huntsville, Alabama 35805
47. J. J. Dorning, Department of Nuclear Engineering and Engineering Physics, Thornton Hall, University of Virginia, Charlottesville, Virginia 22901
48. Lt Richard Engstrom, AFWL/NTCA, Air Force Weapons Laboratory, Kirtland Air Force Base, Albuquerque, New Mexico 87117
49. R. M. Haralick, Department of Electrical Engineering, University of Washington, Seattle, Washington 98195
50. Office of the Assistant Manager for Energy Research and Development, Department of Energy, Oak Ridge Operations, P.O. Box 2001, Oak Ridge, TN 37831

51–60. Office of Scientific and Technical Information, P.O. Box 62, Oak Ridge, Tennessee 37830